Catalysis Letters, Vol. 116, Nos. 1–2, July 2007 (© 2007)
DOI: 10.1007/s10562-007-9093-x

Fabrication of molybdenum carbide catalysts over multi-walled carbon nanotubes by carbothermal hydrogen reduction

Xiaoyun Li, Ding Ma, Limin Chen, and Xinhe Bao*

State Key Laboratory of Catalysis, Dalian Institute of Chemical Physics, Chinese Academy of Sciences, 457 Zhongshan Road,
P.O. Box 110, Dalian 116023, P.R. China

Received 18 March 2007; accepted 18 March 2007

Molybdenum carbide catalysts were successfully prepared using original multi-walled carbon nanotubes (MWCNTs) and nitric acid treated ones as support and carbon source by carbothermal hydrogen reduction from 580 °C to 700 °C. Ammonium heptamolybdate was used as Mo precursor and the effects of oxygen functional groups on MWCNT surface were investigated. TEM and XRD results show that oxygen functional groups act as anchor sites to interact with the Mo oxyanion species during impregnation, which promote the dispersion of Mo precursors. Due to the relatively strong interaction between Mo precursors and MWCNTs, the agglomeration of Mo carbide particles is prevented even when the treatment temperature is as high as 700 °C. Moreover, as the support, modified MWCNTs exhibit better thermal resistances. The temperature (580 °C) for Mo_2C formation over MWCNTs is much lower than that over conventional carbon supports using carbothermal hydrogen reduction. The methylcyclohexane dehydrogenation was used as a probe reaction to test the catalytic performances of the Mo_2C catalysts obtained.

KEY WORDS: molybdenum carbide; carbon nanotubes; surface oxygen groups; molybdenum oxyanion; methylcyclohexane dehydrogenation.

1. Introduction

Mo_2C catalysts have received considerable attention since they show catalytic properties comparable to the noble metals [1–3]. In particular, Mo_2C catalysts are very efficient in some hydrogen-involved reactions, very much similar to Pt, Ir and Rh catalysts [4–12]. However, as native Mo_2C has very small surface areas, to prepare Mo_2C with high surface areas or to make it highly dispersed over support is critical to apply this material into the practice. Normally, some materials with high surface areas such as alumina, zeolite and carbon are used as supports to prepare supported molybdenum carbide catalysts [13–15]. The supported Mo_2C catalysts often exhibit much more active and stable [13,14] than bulk Mo_2C catalysts.

When oxides are used as supports for molybdenum carbide catalysts, alkane or alkene precursors are usually needed as carbon source in the preparation process. On the other hand, carbon materials are promising supports in many Mo_2C-related catalyst systems. Beside the role of support, carbon materials are also able to provide the carbon source for the carbide. Thus the unnecessary carbonaceous depositions are avoided on the surface. Ledoux and Pham-Huu synthesized metallic carbides using the reaction of the vapor of metal oxide with the solid carbon at very high temperature. After reaction, the carbides kept the porous structure of the activated carbon [16]. Using H_2-TPR method, Mordenti *et al.* prepared activated carbon supported Mo_2C successfully, with size of carbide particles around 14 nm [17]. Then Liang *et al.* used carbon with ultrahigh surface areas (>3000 m^2/g) as support and carbon source to synthesize β-Mo_2C [18]. The Mo_2C/C catalysts have been tried in some specific catalytic reactions. For example, Sayag and coworkers compared the performances of Mo_2C supported over carbon black composites and HNO_3 activated ones in indole hydrodenitrogenation reaction [19]. The results showed that HNO_3 treatment increased the dispersion of Mo_2C, and the catalyst obtained exhibited higher activity in the reaction. Monteverdi and coworkers tested the performance of activated carbon supported β-Mo_2C in propene hydrogenation reaction [20]. They observed that the stability of the catalyst depended on the dispersion of the catalyst and the degree of carburization.

As an interesting carbon form, carbon nanotubes (CNTs) have different structural and electronic properties from other carbon materials [21]. However, very limited studies about Mo_2C/CNT catalysts have been reported [22,23]. In the present work, we prepared Mo_2C over original and modified multi-walled carbon nanotubes (MWCNTs) by the method of carbothermal hydrogen reduction. The catalysts obtained were characterized by XRD and TEM. The results show that

---

*To whom correspondence should be addressed.
E-mail: xhbao@dicp.ac.cn

using MWCNTs as carbon source reduces the temperature for the formation of molybdenum carbide. At the same time, the surface oxygen groups anchor the Mo species and promote their dispersion. The methylcyclohexane (MCH) dehydrogenation reaction was chosen to test the catalytic performances of obtained Mo_2C catalysts.

2. Experimental

2.1. MWCNT modification

The original MWCNTs were purchased from Chengdu Organic Chemicals Co., LTD. China. They were denoted as CNTs-O. The nitric acid modification was conducted according to the literature [24]. Briefly, 3 g CNTs-O were suspended in 150 ml 68 wt% nitric acid and refluxed at 140 °C for 15 h. Then, the MWCNTs were filtrated, washed by deionized water till they were neutral and dried at 60 °C. The acquisitions were denoted as CNTs-N. These two kinds of MWCNTs were used as supports to prepare the Mo_2C catalysts.

2.2. Catalyst preparation

The catalyst preparation procedures included two steps. Firstly, the Mo precursor, ammonium heptamolybdate (AHM) was introduced onto the MWCNTs by incipient impregnation method. The weight ratio of molybdenum to the support was 20:100. In brief, appropriate AHM was dissolved in a certain volume of deionized water. Then the solution was added into the support under stirring. After keeping the sample at room temperature for 15 h, it was dried at 60 °C overnight. Secondly, 100 mg drying sample was put into a fix-bed reactor and heated up to a certain temperature (Tr) in 100 ml/min hydrogen flow. Here, four temperatures (500, 580, 630 and 700 °C) were chosen. The heating ramp was from room temperature to 340 °C in 80 min, then 340 °C to Tr at 1 °C/min. The sample was held at Tr for 1 h before cooling down to room temperature in hydrogen flow. Prior to exposure to air, the sample was passivated in a 1% O_2/He (20 ml/min) for 0.5 h.

2.3. Characterization methods

The surface area and pore volume of two supports were measured by nitrogen adsorption at −196 °C, using a Quantachrome autosorb-1 apparatus. Before nitrogen adsorption measurements, the samples were vacuumized at 120 °C for 15 h.

TPD experiments were performed on a quartz U-type reactor equipped with a quadrupole MS (Omini-Star). Prior to the TPD experiment, 50 mg MWCNTs were kept in the helium flow (50 ml/min) for 1 h at ambient temperature to obtain the stable baseline. TPD measurements were done from room temperature to 970 °C with a heating rate of 10 °C/min, with He (50 ml/min) as the carrier gas.

XRD measurements were carried out on a Rigaku D/Max 2500 diffractometer with a Cu kα monochromatized radiation source, operated at 40 kV and 250 mA. Average crystallite size was calculated according to the Scherrer's equation, $D = k\lambda/(\beta \cos\theta)$, where k is a constant related to the shape of the polycrystals (here taken as 0.9), λ is the X-ray wavelength, β is the full-width at half maximum (FWHM) of the respective diffraction peak, θ is the Bragg angle [25].The catalysts treated at different temperature were observed by TEM on Tecnai G^2 spirit apparatus.

2.4. Catalytic tests

The MCH dehydrogenation was carried out under atmospheric pressure in a fixed-bed reactor (quartz, o.d. = 10 mm). Before entering the reactor, the gases (99.999%) were treated with 5A zeolite and deoxidation tubes to remove H_2O and O_2. The flow rate of MCH was controlled by a syringe micropump. Prior to reaction, 100 mg catalyst was *in situ* treated in hydrogen flow (100 ml/min), at the same program as in section 2.2. After the treatment, the temperature was cooled down to 400 °C. The MCH, which was vaporized and mixed with H_2 through a vaporizer, was introduced into the reactor. The flow rate of liquid MCH was 0.01 ml/min and H_2/MCH mole ratio was fixed at 3/1. The effluents were analyzed on-line using a Shimadzu-GC equipped with a 4 m SE-30 column.

3. Results and discussion

3.1. MWCNT properties

It is known that an oxidative treatment by nitric acid will introduce oxygen functional groups onto the surface of carbon materials. The types and amounts of these oxygen groups will change the carbon surface chemistry. In current study, various experimental techniques such as XPS, FT-IR and TPD have been used to characterize the oxygen groups. Herein, TPD is the most popular method, with which surface oxygen groups are assigned according to CO and CO_2 peaks released at different temperature when carbon materials are heated at inert atmosphere [26,27]. In the present study, the oxygen groups of the original and modified MWCNTs were measured by TPD method and the profiles are shown in figure 1. In the case of CNTs-O, absence or very small amount of CO_2 and CO release shows that there are none or very limited carbon-oxygen complexes on the surface. However, after nitric acid treatment (CNTs-N), large amounts of CO_2 and CO release were observed. The total amounts of CO_2 and CO by integrating for two kinds of MWCNTs are presented in table 1. From the data, we can see that after oxidative treatment, the

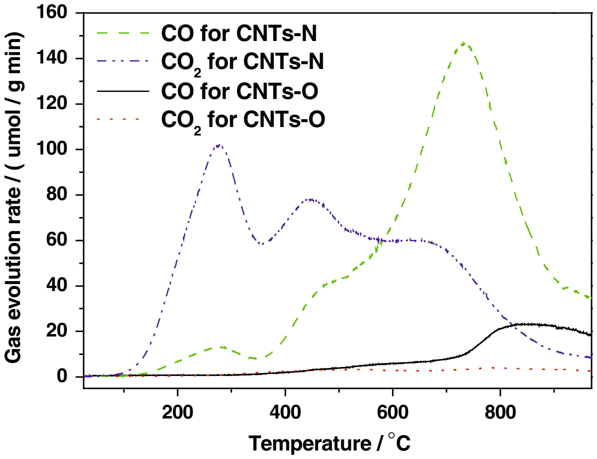

Figure 1. CO- and CO_2-TPD profiles for the original and modified MWCNTs.

Table 1
Physicochemical properties of different MWCNTs

Sample	BET surface area (m^2/g)	Total pore volume (cm^3/g)	Integrated CO and CO_2 evolution	
			CO (mmol/g)	CO_2 (mmol/g)
CNTs-O	172.2	0.403	0.21	0.09
CNTs-N	219.8	0.633	3.26	4.07

amounts of CO_2 and CO increase about 45 and 15 times, respectively. Different surface oxygen groups will decompose at different temperature. For CNTs-N, there are three CO_2 desorption peaks at 275, 450 and 670°C. According to the literature [27], they are assigned to the decomposition of carboxylic, anhydride and lactone groups, respectively. A CO desorption peak at 450°C was observed as well. It comes from the decomposition of anhydride because each anhydride group decomposes one molecule of CO_2 and one of CO. The CO peak at about 730°C is the contribution from the decomposition of two kinds of oxygen groups, phenols and carbonyls-quinones. So we can conclude that, comparing to CNTs-O, a lot of oxygen functional groups such as carboxylic, anhydride, lactone, phenol and carbonyl-quinone are introduced onto the surface of CNTs-N.

The treatment by nitric acid not only introduces oxygen functional groups onto the surface but also opens the tips of tubes [28]. In this case, the tubes of the original MWCNTs are close-ends, while they are opened upon acid treatment. Another evidence of open-ended tubes after treatment is the data of BET surface areas, shown in table 1. The surface area of treated MWCNTs increases about 30% compared to the original ones. It indicates the exposure of inner surface after oxidative treatment. The ratio of external surface area to internal surface area was reported to be about 3 for MWCNTs, which agreed well with present observation [29]. In addition, the adsorption capacities of MWCNTs increase after treatment.

3.2. *Mo oxyanion species adsorption on different MWCNTs during impregnation*

When a lot of oxygen functional groups existed on the surface of MWCNTs, a distinct transformation was that hydrophobic MWCNTs became hydrophilic. In our system, the solution of AHM was used as Mo precursor and the major species in the solution was $Mo_7O_{24}^{6-}$ (pH 5.1). The hydrophilic nature of the modified MWCNTs and the electrostatic interaction between Mo species and MWCNTs benefit anchoring Mo oxyanions onto the interior and exterior surfaces during impregnation. In order to determine it, samples after drying at 60 °C were measured by TEM and XRD. The TEM images are shown in figure 2. For AHM/CNT-N sample, very fine particles (less than 7 nm) are well dispersed on both the external and internal surfaces of the tubes (figure 2B). Instead, the interiors of tubes on AHM/CNTs-O are empty, and some larger molybdenum particles are observed on the external surface (figure 2A).

The XRD patterns of supported AHM catalysts after drying at 60 °C are shown in figure 3. There are some differences in 8–18° regions for AHM on different supports. According to JCPDS reference patterns (PDF numbers: 70-1707, 23-0784 and 23-0785), the XRD peaks at 2θ = 8.97°, 9.65°, 10.20°, 11.40° and 13.65° can be assigned to $(NH_4)_6Mo_7O_{24}$ and its hydrates. The broadened XRD peaks of AHM/CNTs-N show that Mo species are well dispersed on the support, which is in good agreement with TEM result. However, there are some differences of XRD peaks of 2θ = 8.97° and 10.20° for AHM/CNTs-N and 2θ = 9.65°, 11.40° and 13.65° for AHM/CNTs-O. We consider that the oxygen functional groups make the differences.

The behaviors of Mo ion adsorption on alumina, titania and carbon supports had been extensively investigated [30–33]. A strong interaction between Mo ions and surface hydroxyl groups on alumina led to the formation of the complex of Al–O–Mo oxyanions [30,31]. On carbon-based support, the adsorption process becomes more complex as various oxygen groups may get involved. Vissers *et al.* found a chemical reaction between an aryl ether functional group and the molybdenum ion on carbon black by FT-IR [34]. Cruywagen and De Wet also proposed surface complexes formation with oxalate, malate derivatives by interactions between Mo ions and the surface oxygen groups [35]. By XPS and FT-IR analysis, De la Puente *et al.* observed that the complexes originated from the interactions between Mo species and C=O containing functional groups (and ether groups) were formed. The complexes could hinder the Mo mobility in the

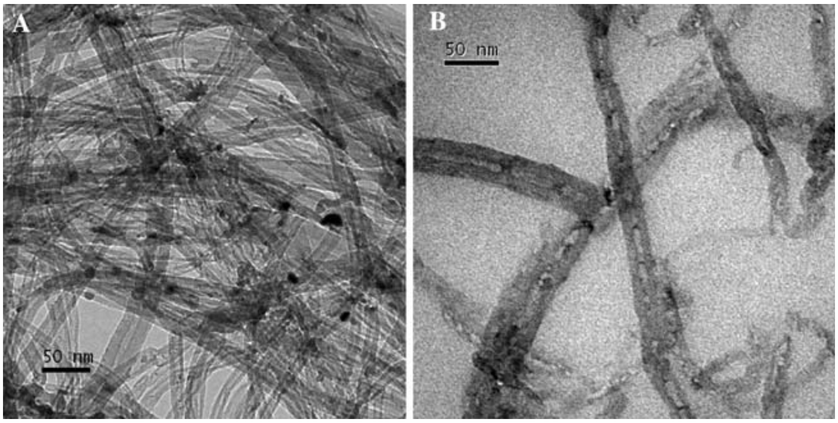

Figure 2. The TEM images of AHM supported over (A) CNTs-O and (B) CNTs-N after drying at 60 °C.

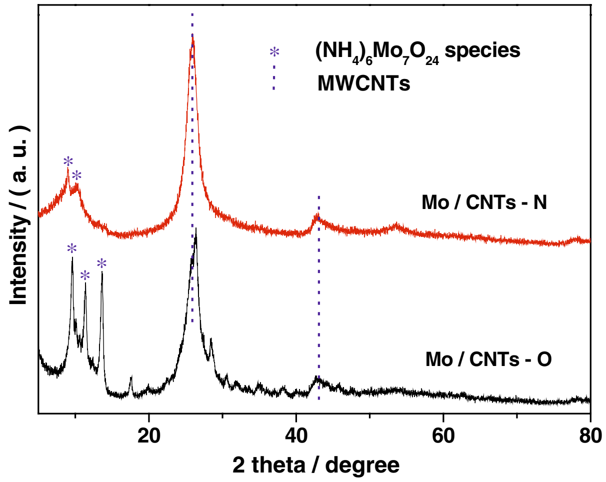

Figure 3. The XRD patterns of AHM/MWCNT catalysts after drying at 60 °C.

activation process [36]. Though the structures of the complexes cannot be determined by XRD experiments, we believe that the strong interaction between Mo oxyanions and oxygen groups on MWCNTs takes place, which improves the dispersion of Mo species.

3.3. *Preparation of Mo_2C catalysts by carbothermal hydrogen reduction*

The Mo catalysts supported over different MWCNTs were treated with hydrogen till 500, 580, 630 and 700 °C, respectively. Their XRD patterns are shown in figure 4. The pattern of Mo/CNT-O sample treated at 500 °C shows a diffraction peak at 40.50°, which is assigned to metallic Mo. At the same temperature, MoO_2 peak at 37.01° was observed on Mo/CNT-N sample. Increasing the treatment temperature to 580, 630 and 700 °C, peaks at 39.39° and 37.97° corresponding to β-Mo_2C with a hexagonal closed packed structure appeared, indicating the successful preparation of Mo_2C/MWCNT catalysts. This demonstrates that supported molybdenum carbide catalysts can be fabricated with MWCNTs as the carbon source. The sharp peaks of Mo_2C over CNTs-O show that the size of the carbide particles is relatively large. Meanwhile, very broad peaks of Mo_2C are observed over catalyst with CNTs-N as the support, indicating that molybdenum carbide is highly dispersed over CNTs-N and the particle size is much smaller. The particle size increases with

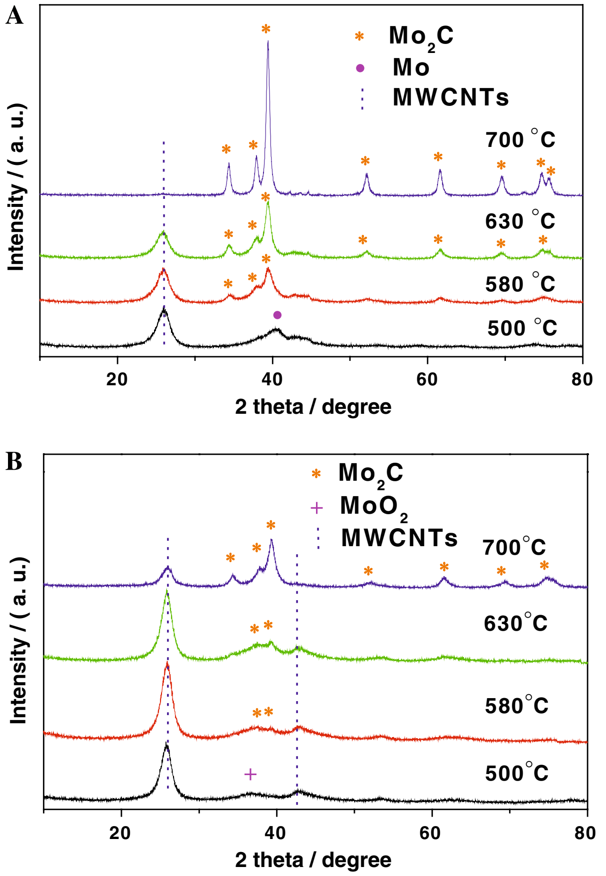

Figure 4. The XRD patterns of Mo catalysts (treated at different temperatures) supported over (A) CNTs-O and (B) CNTs-N.

the increasing treatment temperature, as evidenced by the reduced FWHM. The details about average particle sizes of samples are listed in table 2 (calculated using Scherrer's equation). The results reveal that as the anchor sites surface oxygen groups can prevent Mo_2C particles from agglomeration during heating process.

The reduction processes of Mo species supported over carbon materials by carbothermal hydrogen reduction were reported to include two successive steps [17,18]. Firstly, the Mo precursor was reduced by hydrogen to form MoO_2. Then MoO_2 was carburized by CH_x species evolved from carbon support to form Mo_2C. According to this mechanism, no metallic Mo was involved. This is not accordant with our present results. There are two possible explanations. For original MWCNTs, Mo precursors can be reduced by H_2 at lower temperature because of their weak interaction with tubes. When MoO_2 is obtained, there is not enough CH_x to react with it because the temperature is not enough high to produce CH_x. Therefore MoO_2 is directly reduced to Mo. On the other hand, we noticed that the mechanism in the literatures was obtained by analyzing H_2 or H_2O peaks in TPR profiles as the Mo species were difficult to be observed by XRD because of low loading and high dispersion of Mo species over carbon. Possibly, there are two superposed peaks, which are difficult to be distinguished. If this is true, the process of MoO_2 to Mo and then to Mo_2C is reasonable in our study. Detailed study on the formation mechanism of Mo_2C over MWCNTs is still in progress. Another interesting thing is, in the present case, the Mo_2C can be successfully prepared at 580 °C over MWCNTs. However, it formed at 700 °C or even higher temperature on other carbon supports such as carbon black and activated carbon according to the literatures [17–19]. It is well known that CNTs have special properties, and under certain condition, can accelerate some specific reactions [24]. Maybe this is the reason for the lower temperatures of Mo_2C formation over MWCNTs than that over other carbon materials. It should be noted that during the preparation process, MWCNTs are used as the support as well as the carbon source. So very high temperature (higher than 700 °C) may destroy the structure of carbon support and carbide particles grow larger. This can be seen from XRD patterns (figure 4). The intensities of carbide peaks increase and the intensity of the peak at 26.06° decreases dramatically.

To estimate the average particle sizes of Mo/MWCNTs, TEM is carried out on all catalysts. Among them, the images of samples treated at 580 and 700 °C are shown in figure 5. Average particle sizes of samples are listed in table 2. For the sample of Mo_2C/CNTs-O treated at 580 °C, we can see that there are a few large particles about 13–15 nm over the support. At the same time, a small amount of small particles about 2–4 nm can be observed to cling on the walls of the tubes. However, after treated at 700 °C, severe conglomeration took place. As shown in figure 5(C), large aggregations of molybdenum carbide particles dominate, which even makes it difficult to determine the individual particle size. Instead, over CNTs-N, particles are well distributed inside and outside the tubes even at 700 °C. The carbon source of carbide comes from MWCNTs. As shown in figure 5(B) and (D), though the structures of tube cavities are kept, some grooves on walls can be observed around the Mo_2C particles. In the case of Mo_2C/CNTs-O, as very large Mo_2C particles are formed, the tubes are destroyed severely. It is consistent with the XRD result.

3.4. MCH dehydrogenation reaction using Mo/MWCNT catalysts

The Mo/MWCNT catalysts were in situ treated by H_2 at 500, 580, 630 and 700 °C, respectively. Then the temperature was cooled down to 400 °C under hydrogen flow and the mixture of MCH and hydrogen was introduced into the reactor. The catalytic performances of all catalysts have the similar behaviors along with the reaction time. The MCH conversions at 5, 80 and 200 min are shown in table 3. There is a prominent deactivation on all catalysts in the initial reaction period. It is well known that toluene is the precursor for carbonaceous deposit. The active sites of catalysts are masked by carbonaceous product, which is the major cause of deactivation. This phenomenon is also observed on Pt and Pd supported catalysts [37].

Table 2

The crystal phase and average particle size of Mo catalysts

Sample	Mo/CNTs-O				Mo/CNTs-N			
	500 °C	580 °C	630 °C	700 °C	500 °C	580 °C	630 °C	700 °C
Crystal phase	Mo	β-Mo_2C	β-Mo_2C	β-Mo_2C	MoO_2	β-Mo_2C	β-Mo_2C	β-Mo_2C
D_1 (nm)[a]	3.75	7.83	11.12	18.06	3.46	3.02	4.93	8.14
D_2 (nm)[b]	3.7	6.0	9.0	–	3.4	3.0	4.5	5.4

[a] Average particle diameter calculated by Scherrer's equation: $D = k\lambda/(\beta\cos\theta)$, (where k is related to the shape of the polycrystals, λ is the X-ray wavelength, β is the full-width at half maximum (FWHM) of the respective diffraction peak, θ is the Bragg angle).

[b] Average particle diameter estimated from TEM images.

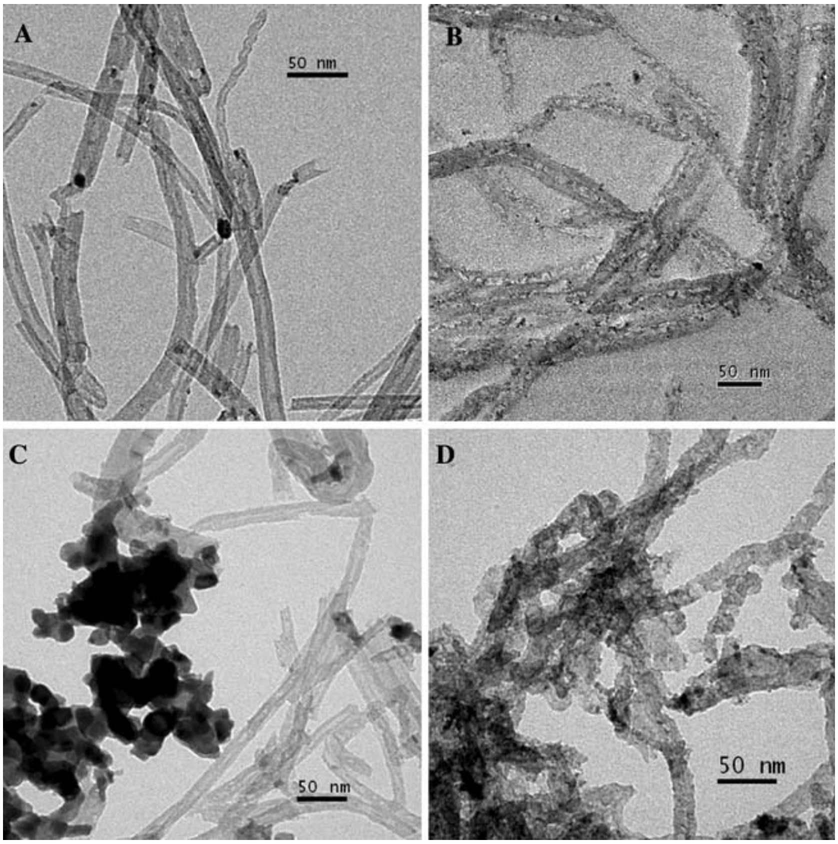

Figure 5. The TEM images of Mo_2C catalysts supported over different MWCNTs after treated in hydrogen flow at different temperatures: (A) Mo_2C/CNTs-O treated at 580 °C; (B) Mo_2C/CNTs-N treated at 580 °C; (C) Mo_2C/CNTs-O treated at 700 °C; (D) Mo_2C/CNTs-N treated at 700 °C.

Table 3

Catalytic activity of the Mo/MWCNT catalysts for the MCH dehydrogenation reaction at 400 °C

Catalyst		MCH conversion (%)			Specific activity[a] (mmol h^{-1} m^{-2})
Support	Tr (°C)	5 min	80 min	200 min	
CNTs-O	500	50.6	26.1	16.0	1.18
	580	66.6	24.8	16.0	2.45
	630	64.9	22.5	16.4	3.47
	700	59.8	20.9	15.7	–
CNTs-N	500	47.5	21.6	15.1	0.47
	580	81.4	31.4	23.4	1.50
	630	73.1	23.7	18.6	1.70
	700	70.0	22.9	17.1	1.86

[a] Specific activity of catalyst calculated based on MCH converted per hour per m^2 of Mo species (reaction carried out at 400 °C and the time on steam is 5 min). The population of surface Mo species (including Mo_2C, Mo and MoO_2) was calculated according to the size distribution from TEM image (supposing those particles are spherical).

The initial conversion of MCH on Mo_2C is always higher than ones on Mo and MoO_2 catalysts. Considering the influence of the particle size, we calculated the moles of MCH converted per hour per m^2 of metal or metal carbide to compare the specific activities of catalysts. From table 3, we conclude that Mo_2C is more effective than Mo and MoO_2 in this dehydrogenation reaction. For Mo_2C catalysts, the specific activity increases with increasing the treatment temperature thus the increase of particle sizes.

4. Conclusions

Oxygen functional groups were introduced onto the MWCNT surface by nitric acid treatment. The existence of the oxygen groups changed MWCNT surface chemistry and promoted the dispersion of Mo oxyanions during impregnation. β-Mo_2C catalysts supported over original and modified MWCNTs were successfully prepared by carbothermal hydrogen reduction. The MWCNTs provide the carbon source for the formation of molybdenum carbide as well as acting as the support. The temperature for Mo_2C formation over MWCNTs is much lower than that over conventional carbon supports by carbothermal hydrogen reduction method. The surface functional groups play a critical role in anchoring the molybdenum species.

In the MCH dehydrogenation reaction, it has been observed that Mo_2C is more active than Mo and MoO_2 catalysts. The activity of Mo_2C catalysts increases with increasing the treatment temperature.

Acknowledgements

We are grateful for the financial support of the National Natural Science Foundation of China (Grant No. 90206036) and the Ministry of Science and Technology of China through the National Key project of Fundamental Research (Grant No. 2005CB221405). We also thank referees for the helpful suggestions.

References

[1] R.B. Levy and M. Boudart, Science 181 (1973) 547.

[2] S.T. Oyama, Catal. Today 15 (1992) 179.

[3] J.G. Chen, Chem. Rev. 96 (1996) 1477.

[4] C. Bouchy, I. Schmidt, J.R. Anderson, C.J.H. Jacobsen, E.G. Derouane and S.B. Derouane-Abd Hamid, J. Mol. Catal. A 163 (2000) 283.

[5] J.S. Lee, S. Locatelli, S.T. Oyama and M. Boudart, J. Catal. 125 (1990) 157.

[6] F. Solymosi, R. Nemeth, L. Ovari and L. Egri, J. Catal. 195 (2000) 316.

[7] M. Nagai, K. Oshikawa, T. Kurakami, T. Miyao and S. Omi, J. Catal. 180 (1998) 14.

[8] J.S. Lee, M.H. Yeom, K.Y. Park, I.S. Nam, J.S. Chung, Y.G. Kim and S.H. Moon, J. Catal. 128 (1991) 126.

[9] A.P.E. York, J.B. Claridge, A.J. Brungs, S.C. Tsang and M.L.H. Green, Chem. Commun (1997) 39.

[10] J. Patt, D.J. Moon, C. Phillips and L. Thompson, Catal. Lett. 65 (2000) 193.

[11] P.D. Costa, C. Potvin, J.M. Manoli, J.L. Lemberton, G. Perot and G. Djega-Mariadassou, J. Mol. Catal. A 184 (2002) 323.

[12] C. Sayag, S. Suppan, J. Trawczynski and G. Djega-Mariadassou, Fuel Process Technol. 77–78 (2002) 261.

[13] M. Tsuji, T. Miyao and S. Naito, Catal. Lett. 69 (2000) 195.

[14] A.J. Brungs, A.P.E. York, J.B. Claridge, C. Marquez-Alvarez and M.L.H. Green, Catal. Lett. 70 (2000) 117.

[15] F. Solymosi and A. Szechenyi, J. Catal. 223 (2004) 221.

[16] M.J. Ledoux and C. Pham-Huu, Cattech 5 (2001) 226.

[17] D. Mordenti, D. Brodzki and G. Djega-Mariadassou, J. Solid State Chem. 141 (1998) 114.

[18] C.H. Liang, P.L. Ying and C. Li, Chem. Mater. 14 (2002) 3148.

[19] C. Sayag, M. Benkhaled, S. Suppan, J. Trawczynski and G. Djega-Mariadassou, Appl. Catal. A 275 (2004) 15.

[20] S. Monteverdi, M. Mercy, S. Molina, M.M. Bettahar, S. Puricelli, D. Begin, F. Mareche and F. Furdin, Appl. Catal. A 230 (2002) 99.

[21] P. Serp, M. Corrias and P. Kalck, Appl. Catal. A 253 (2003) 337.

[22] H. Park, M.H. Kim, Y.K. Hwang, J.S. Chang and Y.U. Kwon, Chem. Lett. 34 (2005) 222.

[23] Z.H. Yang, P.J. Cai, L. Shi, Y.L. Gu, L.Y. Chen and Y.T. Qian, J. Solid State Chem. 179 (2006) 29.

[24] W. Chen, X.L. Pan, M.G. Willinger, D.S. Su and X.H. Bao, J. Am. Chem. Soc. 128 (2006) 3136.

[25] B.D. Cullity, *Elements of X-ray Diffraction*, 2nd ed. (Addison Wesley Publishing Co., Menlo Park, CA, 1978) p. 102.

[26] J.L. Figueiredo, M.F.R. Pereira, M.M.A. Freitas and J.J.M. Orfao, Carbon 37 (1999) 1379.

[27] A.E. Aksoylu, M. Madalena, A. Freitas, M.F.R. Pereira and J.L. Figueiredo, Carbon 39 (2001) 175.

[28] H. Hiura, T.W. Ebbesen and K. Tanigaki, Adv. Mater. 7 (1995) 275.

[29] Z.J. Li, M. Kruk, M. Jaroniec and S.K. Ryu, J. Colloid Interf. Sci. 204 (1998) 151.

[30] F.M. Mulcahy, M.J. Fay, A. Proctor, M. Houalla and D.M. Hercules, J. Catal. 124 (1990) 231.

[31] J.A. Bergwerff, T. Visser, B.R.G. Leliveld, B.D. Rossenaar, K.P. Jong and B.M. Weckhuysen, J. Am. Chem. Soc. 126 (2004) 14548.

[32] N. Spanos, H.K. Matralis, C. Kordulis and A. Lycourghiotis, J. Catal. 136 (1992) 432.

[33] J.M. Solar, F.J. Derbyshire, V.H.J. De Beer and L.R. Radovic, J. Catal. 129 (1991) 330.

[34] J.P.R. Vissers, S.M.A.M. Bouwens, V.H.J. De Beer and R. Prins, Carbon 25 (1987) 485.

[35] J.J. Cruywagen and H.F. De Wet, Polyhedron 7 (1988) 547.

[36] G. de la Puente, A. Centeno, A. Gil and P. Grange, J. Colloid Interf. Sci. 202 (1998) 155.

[37] Y.G. Wang, N. Shah and G.P. Huffman, Energy Fuel 18 (2004) 1429.